## How to get more out of a clinically feasible 64 Gradient dMRI Acquisition: Multi-Shell versus Single-Shell

Rutger Fick<sup>1</sup>, Mauro Zucchelli<sup>2</sup>, Gabriel Girard<sup>1,3</sup>, Gloria Menegaz<sup>2</sup>, Maxime Descoteaux<sup>3</sup>, and Rachid Deriche<sup>1</sup>

<sup>1</sup>Team Athena - INRIA, Sophia Antipolis, Alpes Maritimes, France, <sup>2</sup>University of Verona, Verona, Italy, <sup>3</sup>Sherbrooke Connectivity Imaging Lab (SCIL), Computer Science Department, Quebec, Canada

**PURPOSE** – For clinical applications the number of diffusion MRI (dMRI) samples that can be obtained is often limited by scanner time and patient comfort. For this reason one often uses short scanning protocols that acquire just 32 or 64 gradient directions using a single b-value to obtain diffusion measures such as the fractional anisotropy from Diffusion Tensor Imaging (DTI)<sup>1</sup> or to estimate the white matter orientation using Constrained Spherical Deconvolution (CSD)<sup>2</sup>. Using 3D-SHORE<sup>3</sup> and MAP-MRI<sup>4</sup>, we show that by spreading the same number of dMRI samples over different b-shells (sampling angularly and radially) we can estimate not only the directionality of the white matter using the ODF, but also the radially dependent higher order diffusion measures that SHORE and MAP-MRI provide. This approach lends itself well for situations where acquisition time is limited, and is therefore particularly well suited for clinical applications.

**METHODS** – To fit the diffusion signal we use the recent 3D Simple Harmonic Oscillator based reconstruction and estimation (3D-SHORE³) and Mean Apparent Propagator MRI (MAP-MRI⁴) bases. Both these bases describe the signal and the diffusion propagator efficiently as a summation of orthogonal basis functions, where the signal and propagator are related through a Fourier transform. In fact, both bases are extensions of the 1D-SHORE basis, where 3D-SHORE uses the product of a 1D-SHORE⁵ and a spherical harmonics basis, while MAP-MRI consists of a product of three orthogonal 1D-SHORE bases. Both are scaled proportionally to the diffusivity of the data, although 3D-

SHORE is scaled isotropically and MAP-MRI is scaled anisotropically relative to the diffusivity in each basis direction.

We evaluate these bases both in terms of fiber crossing angle recovery using the Orientation Density Function (ODF) and microstructure recovery under clinically feasible setting. In terms of crossing angle we compare 3D-SHORE and MAP-MRI with the classical Constrained Spherical Deconvolution (CSD) model². We use the multi-tensor model in Dipy $^6$  to simulate a 90, 60 and 45 degree crossing using a total of 64 samples, spread over 1 shell at b=3000 for CSD or spread equally over 3 shells at b={1000,2000,3000} for 3D-SHORE and MAP-MRI. To evaluate microstructure recovery we simulate the restricted intra-axonal diffusion signal using the cylinder model $^5$ , which adheres to the small gradient pulse approximation ( $\delta \approx 0$ ) and

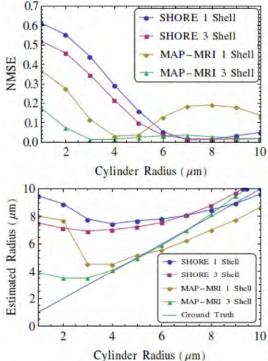
long diffusion time ( $\Delta \gg \delta$ ). These conditions allow us to link the Return-To-Axis Probability (RTAP<sup>4</sup>), expressed in fitted 3D-SHORE or MAP-MRI coefficients, to the cross-sectional area (CSA) of a cylindrical pore<sup>4</sup>. Assuming a uniform radii distribution we then compute the cylinder radius from the CSA.

**RESULTS** – In the table we shows the results of the multi-tensor<sup>6</sup> experiment, where we generated a 90, 60 and 45 degree crossing at SNR=20 using 300 different noise generations. We see that CSD using the single shell data and SHORE on the multi-shell data have similar crossing recovery, with CSD having a slightly lower standard deviations. Interestingly, we find that for angles smaller than 90<sup>0</sup> MAP-MRI significantly underestimates the crossing angle.

When we compute the Normalized Mean Squared Error (NMSE) of the SHORE or MAP-MRI signal fitting with respect to the 10-shell ground truth signal (1290 gradients, b<sub>max</sub>=10000) we find that MAP-MRI has lower errors compared to SHORE for lower axon radii, and that sampling multiple shells further reduces the error compared to sampling just a single shell. With respect to axon radius recovery we find a similar trend, where MAP-MRI is able to recover smaller axon radii compared to 3D-SHORE, and again sampling multiple shells further improves the result.

**DISCUSSION & CONCLUSION** – In this work we show that by spreading diffusion samples on multiple shells instead of one we gain access to both the accurate recovery of crossing angles using 3D-SHORE and microstructural features such as the axon radius using MAP-MRI. We observe that MAP-MRI has the lowest fitting error and most accurate microstructure recovery of the given methods, but at the same time significantly underestimates crossing angles smaller than 90 degrees compared to both 3D-SHORE and the classical CSD. We find

GT	CSD	SHORE	MAP-MRI
$90^{0}$	$89.9^{0} \pm 1.9^{0}$	$89.6^{\circ} \pm 5.5^{\circ}$	$89.9^{\circ} \pm 5.0^{\circ}$
$60^{0}$	$58.8^{\circ} \pm 2.0^{\circ}$	$58.1^{\circ} \pm 5.0^{\circ}$	$43.2^{\circ} \pm 3.0^{\circ}$
$45^{0}$	$40.2^{0} \pm 9.2^{0}$	$46.7^{0} \pm 10.2^{0}$	$30.3^{0} \pm 2.5^{0}$



that the improved signal fitting and underestimation of the crossing angles is proportional to the anisotropy of the scaling used in MAP-MRI's basis functions (result not shown), making MAP-MRI's excellent microstructure recovery a double-edged sword. While this phenomenon deserves further exploration, here we have shown that by simply spreading the available samples over multiple shells we can still accurately recover crossing angles and we enable microstructural imaging in clinically feasible settings.

REFERENCES – [1] P. Basser et al. Journal of Magnetic Resonance. 1994, 103: 247–254 [2] J-D. Tournier et al. Neuroimage 2007, 4: 1459-1472 [3] E. Ozarslan et al. Proc Intl Soc Mag Reson Med. 2009, 17: 1396 [4] E. Ozarslan et al. Neuroimage. 2013; 78: 16:32. 1628-1634. [5] E. Ozarslan et al. Excursions in Harmonic Analysis, Volume 2 2013, 373-399 [6] E. Garyfallidis et al. 17th OHBM 2011 [7] S.L. Merlet et al. Medical Image Analysis. 2013; 17: 556-572.